DOI: https://doi.org/10.14311/TPFM.2026.033

EFFECT OF SURFACE ROUGHNESS ON VORTEX SHEDDING IN THE WAKE OF A CIRCULAR CYLINDER IN A SUBCRITICAL REGIME

V. Uruba[1, 2], P. Procházka[1]

[1] Institute of Thermomechanics of the Czech Academy of Sciences, Dolejškova 5, 182 00 Praha 8, CR

[2] Department of Power System Engineering, Faculty of Mechanical Engineering, University of West Bohemia, Universitní 8, 301 00 Plzeň, CR

Abstract

An experimental study of vortex shedding in the wake of a circular cylinder at a subcritical Reynolds number of approximately 5 000 is presented, with emphasis on the influence of surface roughness. Planar particle image velocimetry (PIV) measurements were performed for a smooth cylinder and for a cylinder with uniformly distributed sand-grain roughness. Mean flow statistics show that surface roughness significantly reduces the size of the recirculation region and increases turbulence intensity in the near wake. The unsteady wake dynamics were analyzed using Oscillation Pattern Decomposition (OPD), which allows identification of the dominant vortex-shedding mode and its higher harmonics. The results indicate a systematic decrease in Strouhal number for the rough cylinder compared with the smooth reference case. Phase-aligned OPD mode topologies further reveal increased streamwise spacing of vortical structures in the rough-surface wake. The study demonstrates that surface roughness has a measurable effect on vortex shedding characteristics even in the subcritical flow regime.

Keywords: circular cylinder, wake, vortex shedding, surface roughness, OPD

1 Introduction

Flow past a circular cylinder is a canonical problem in fluid mechanics and a fundamental model for understanding bluff-body wakes, unsteady aerodynamic loading, and vortex-induced vibrations. Alternating vortex shedding in the cylinder wake generates fluctuating lift forces and narrow-band velocity and pressure spectra, which are of central importance in applications such as heat-exchanger tube banks, offshore risers, bridge cables, and slender structural elements. Despite its geometric simplicity, the circular-cylinder wake shows strong dependence on Reynolds number, boundary-layer state, and surface condition, making it particularly sensitive to small perturbations.

At a Reynolds number of approximately 5 000, the flow lies within the subcritical regime. For a smooth circular cylinder, the boundary layer remains laminar up to separation, and transition to turbulence occurs primarily in the separated shear layers and the near wake. The wake is characterized by a well-defined Kármán vortex street with a dominant shedding frequency, commonly expressed as the Strouhal number. Early experiments demonstrated that periodic vortex shedding persists over a wide range of subcritical Reynolds numbers, even as the wake undergoes progressive transition and breakdown downstream [1]. Subsequent investigations revealed that, beyond relatively low Reynolds numbers, the wake becomes intrinsically three-dimensional, with spanwise variations influencing vortex formation, coherence, and unsteady loading [2].

Comprehensive reviews of circular-cylinder flow emphasize that, in the subcritical regime, wake dynamics are governed by the interaction between laminar boundary-layer separation, shear-layer instability, and near-wake feedback mechanisms [2,3]. Although the Strouhal number varies only weakly with Reynolds number in the range from approximately 1 000 to 10 000, the amplitude, coherence, and spectral bandwidth of the fluctuating lift forces change significantly. Norberg [4,5] demonstrated that, even within the subcritical regime, variations in wake organization and vortex coherence strongly affect unsteady loading, underscoring that the shedding frequency alone is insufficient to characterize vortex shedding dynamics fully.

Surface roughness represents an unavoidable and practically relevant perturbation in real applications, arising from manufacturing tolerances, corrosion, biofouling, icing, or deliberate surface treatments. Its influence on cylinder aerodynamics has been studied extensively at higher Reynolds numbers, where roughness can promote early boundary-layer transition, modify separation, and lead to pronounced changes in drag and wake structure. The classical experiments of Achenbach [6] quantified the influence of distributed roughness on pressure distribution and separation behavior and introduced roughness parameters that remain widely used. These studies, however, are primarily concerned with the critical and supercritical regimes, where roughness-induced boundary-layer transition dominates the flow response.

In contrast, the role of surface roughness in the subcritical regime at Reynolds numbers of order 5 000 is more subtle and considerably less documented. At these Reynolds numbers, roughness is generally insufficient to trigger fully turbulent boundary layers before separation. Nevertheless, it can still alter the separation angle, perturb the separated shear layers, and modify the feedback between near-wake vortices and the body. These effects may influence not only the vortex shedding frequency, but also the spatial organization and coherence of the wake. Numerical simulations at comparable Reynolds numbers (e.g. Re ≈ 3 900 in [7]) indicate that surface roughness can produce measurable changes in wake topology, vortex formation length, and force fluctuations, even well below the critical regime. Experimental evidence in this Reynolds-number range remains limited and shows trends that depend strongly on roughness scale, distribution, and measurement methodology.

As a result, a consistent experimental picture of how distributed surface roughness affects vortex shedding in the subcritical regime is still lacking. In particular, there is little experimental work that directly links roughness-induced modifications of the mean wake to changes in vortex shedding frequency and spatial organization under well-controlled subcritical conditions. Given the inherently three-dimensional nature of the wake in this Reynolds-number range, an improved understanding of how surface roughness modifies near-wake dynamics is essential for reliable prediction of unsteady loading on practical, non-smooth cylindrical structures.

The objective of the present study is therefore to investigate the effect of uniformly distributed surface roughness on vortex shedding in the wake of a circular cylinder at a Reynolds number of approximately 5 000. Planar PIV measurements are used to characterize both mean-flow modifications and unsteady wake dynamics for a smooth cylinder and a roughened counterpart. Oscillation Pattern Decomposition (OPD) is employed to identify the dominant vortex-shedding mode and its higher harmonics, and to analyze changes in shedding frequency and spatial vortex organization. By focusing on a well-defined subcritical Reynolds number, the study aims to clarify the mechanisms by which surface roughness alters the separation–shear-layer–wake interaction governing vortex shedding, and to provide experimental evidence of roughness-induced changes in vortex spacing and Strouhal number in this regime.

2 Experimental setup

The experiments were carried out in the low-velocity blow-down wind tunnel, with a test section measuring 250 mm x 250 mm in cross-section and 600 mm in length. The turbulence intensity at a velocity of 5 m/s was about 0.3%, as measured by the hot-wire technique. Measurements were made well inside the regular velocity field, far from walls, where velocity irregularity was below 0.2% of the nominal velocity.
Reynolds and Strouhal numbers Re and Sr are defined as usual:

$$\mathrm{Re} = \frac{U_i \cdot D}{\nu}, \quad \mathrm{Sr} = \frac{f \cdot D}{U_i}, \tag{1}$$

where U_i is the inlet velocity, D is the cylinder diameter, f is the frequency, and ν is the air kinematic viscosity.

Two cases are to be presented, characterized by different surface roughness. The “r0” case is for the smooth surface, while “r2” is for the rough surface. As the models are made of an aluminum tube with a nominal diameter of 15 mm and a rough surface fabricated by attaching sand grains with a mean size of 0.25 mm, the models have different diameters D. The body's exact shape is scanned using the GOM 3D scanner. The air velocity U_i was 5 m/s in both cases. The cases are characterized in Table 1.

Table 1: Cylinders

Case	D [mm]	k [mm]	k/D [1]	Re [1]
r0	15.06	0	0	5 140
r2	16.02	0.25	0.0156	5 470

The Reynolds number differs slightly due to the different diameters.

The dimensionless coordinates (x,y,z) are defined as multiples of the cylinder's diameter D. The dimensionless velocities are multiples of the inlet velocity U_i.

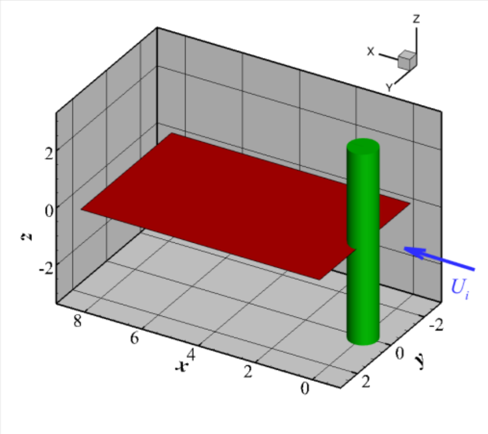

Figure 1: Experiment setup.

The classical planar PIV experimental technique was used. The plane of measurement is shown in red in Fig. 1. The measurement apparatus consists of a laser and a CMOS camera from Dantec Company. The laser is a New Wave Pegasus Nd:YLF double head with a wavelength of 527 nm, a maximum frequency of 10 kHz, and a shot energy of 10 mJ (at 1 kHz); thus, the corresponding power is 10 W per head. The VEO 410 camera, with a resolution of 1 280 x 800 pixels, can acquire double snaps at up to 2 500 Hz (full resolution). The internal memory is 16 GB, enabling the storage of 4,000 double snapshots. The data were acquired and post-processed using DynamicStudio and Tecplot.

Statistics were evaluated from data acquired at 100 Hz, with 1 000 double snapshots representing 10 s in real time. The dynamical measurement data consists of 4 000 double snapshots acquired at 2 kHz, thus representing 2 s of real time. The Safex particle generator in the form of oil droplets was used; the mean particle diameter was 1 µm.

Only in-plane velocity components u and v in the x and y directions were evaluated. Expected ambiguity of the evaluated instantaneous velocities is of order 2-3% of the magnitude, while the precision of mean velocities is better than 1%; for detailed error analysis, see e.g. [8].

3 Results

We present all cases in dimensionless representation: coordinates in multiples of the cylinder diameter and velocities in multiples of the inlet velocity.

The smooth surface (r0) and the rough (r2) cases are to be compared. Each result is presented to compare the smooth-cylinder surface r0 on the left with the rough-cylinder surface r2 on the right.

3.1 Statistics

First, the time-mean characteristics are to be presented. The statistics were evaluated from 10 s records.
In Fig. 2, the vector fields are shown, and vector lines are added arbitrarily to visualize the flow topology.

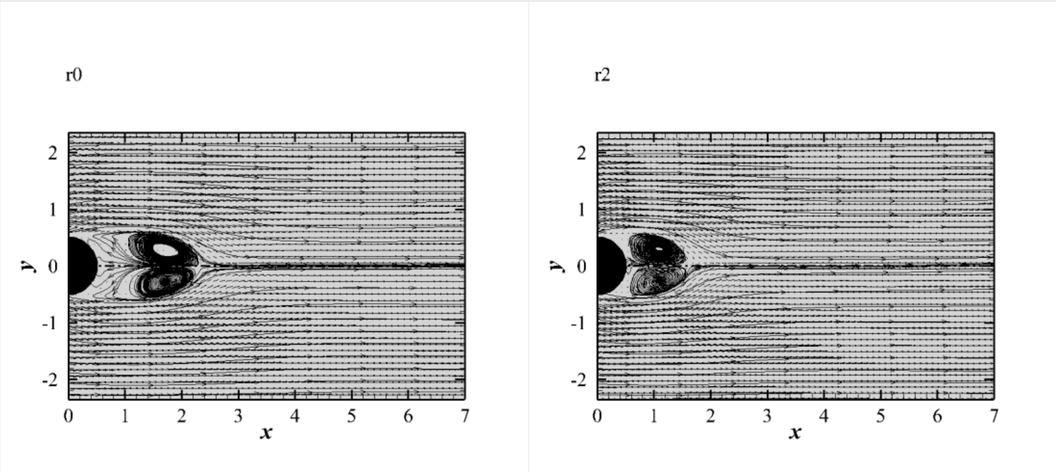

Figure 2: Mean velocity vector fields (smooth surface left, rough right)

In Fig. 3, the distribution of the streamwise mean velocity component is depicted. A white line delimits the back-flow region characterized by a negative mean streamwise velocity component.

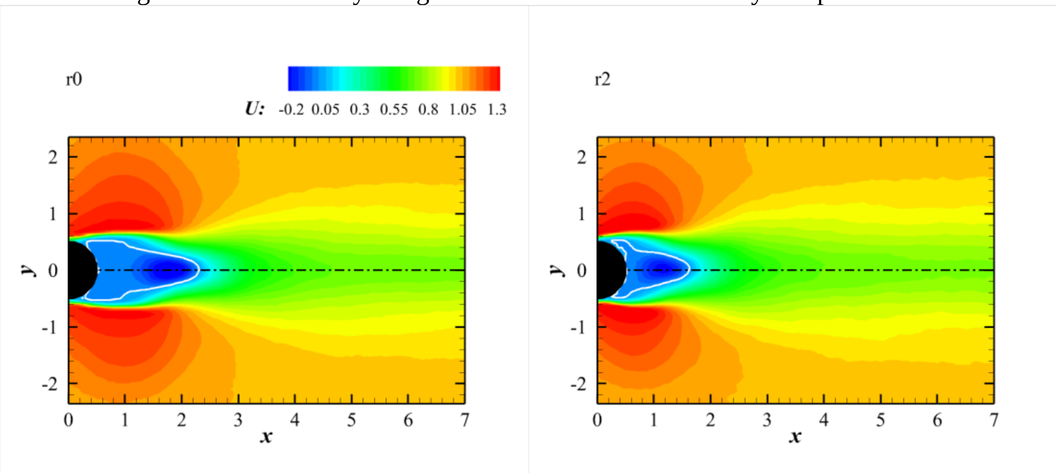

Figure 3: Mean streamwise velocity component distributions (smooth surface left, rough right)

The results in Figs. 2 and 3 clearly show the effect of surface roughness on the size of the backflow region. Surface roughness substantially reduces the size of this region by about 37%.

The rough surface of the cylinder clearly determines the size of the backflow region. The rough surface significantly shortens the backflow region.

Next, the fluctuation characteristics were evaluated. The turbulence kinetic energy *TKE* and correlation coefficient *C* were defined in the following way:

$$TKE = \frac{1}{2}\left(\left\langle u'^2 + 2v'^2 \right\rangle\right), \quad C = \frac{\langle u'v' \rangle}{\sqrt{\langle u'^2 \rangle \langle v'^2 \rangle}}, \qquad (2)$$

where $\langle . \rangle$ is ensemble averaging, u' and v' are dimensionless velocity fluctuations in x and y directions, respectively.

In Figs. 4 and 5 the *TKE* and correlation coefficient distributions are shown, respectively.

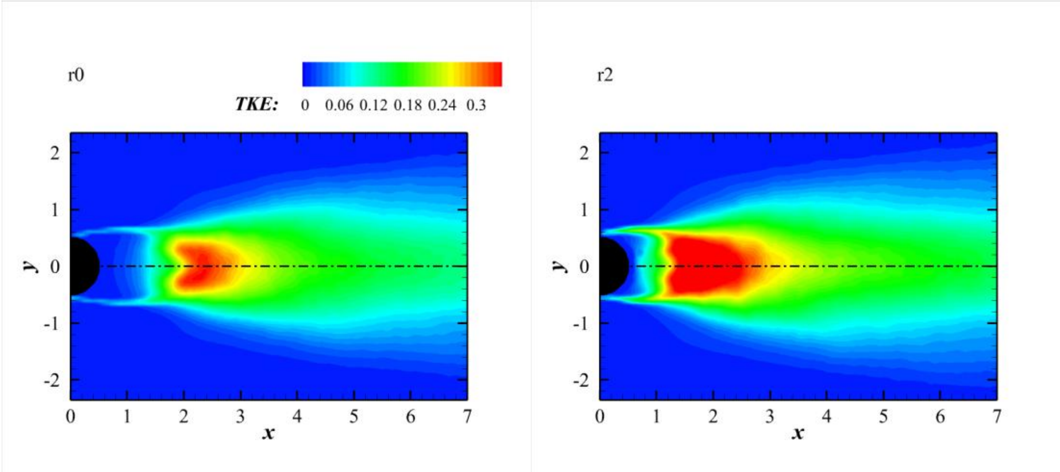

Figure 4: TKE distributions (smooth surface left, rough right)

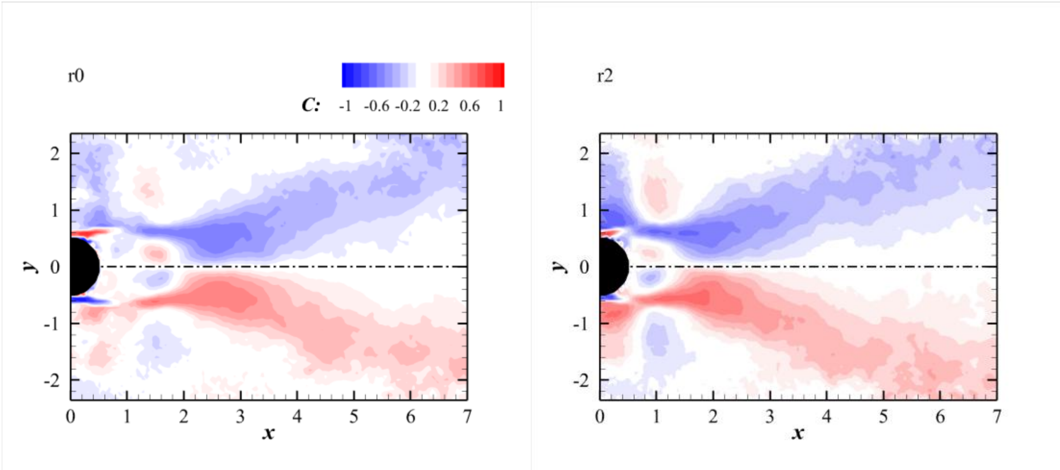

Figure 5: Correlation coefficient distributions (smooth surface left, rough right)

Obviously, there is much higher turbulence activity in the wake of the rough-surface cylinder, and the perturbed region is much larger.

The nonzero correlation coefficient value indicates turbulence production due to the phase link between the velocity fluctuation components. In this indicator, both cases are similar.

3.2 Dynamics

From the spatio-temporal OPD analysis, the three essential modes are evaluated. They correspond to 3 harmonic components of the basic pseudo-periodic process that characterize von Karman street dynamics. The OPD modes for a smooth cylinder were already presented in [9]. Now we will study the effect of cylinder surface roughness. The Strouhal numbers characterizing these modes are listed in Table 2.

Table 2: Strouhal numbers

OPD m	1	2	3
r0	0.209	0.613	0.395
r2	0.202	0.595	0.365

The Strouhal numbers were also evaluated using the hot-wire technique, see [10].

OPD mode 1 represents the basic vortex street characterized by Sr ≈ 0.2. OPD mode 2 corresponds to the 3rd harmonics of the basic process, while OPD 3 corresponds to the 2^{nd} harmonics. The frequencies in the rough-cylinder wake are systematically lower than those for the smooth surface.

The topology mode M is a velocity vector structure that appears as a complex entity consisting of two parts: the real part M_r and the imaginary part M_i. The cyclostationary behavior is characterized by changing phase during a time period in the following manner: the phase sequence: 0, π/2; π; 3π/2; π, and the pattern sequence: M_r; M_i; - M_r; - M_i. More on the OPD technique, see e.g. [11].

The real and imaginary topologies for the case of a smooth cylinder are presented in Fig. 6.

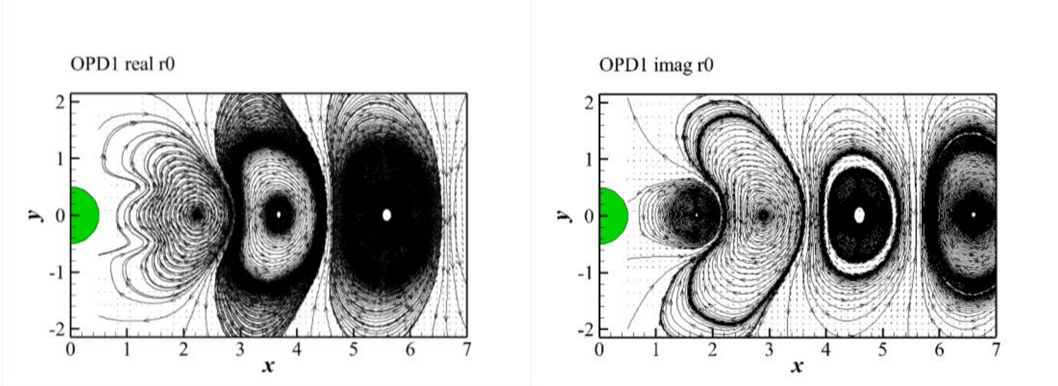

Figure 6: Real (left) and imaginary (right) parts of OPD 1 topology for a smooth cylinder

The mode topology suggests the train of vortices with centers on the axis moving downstream. The intermediate phase angles mode topology is defined as a linear combination of the real and imaginary parts in the following manner:

$$M = M_r \cos\varphi + M_i \sin\varphi \,, \tag{3}$$

where φ is the phase angle.

The mode comparison will be performed for the phase angle appropriately defined for each case.

In general, the OPD modes are evaluated for an arbitrary phase. So, if we want to compare two OPD modes evaluated from different data sets, we should convert the topologies to a common phase, since the phase angle varies from case to case. If we assume the mode has a periodic wave character, a single, appropriately chosen phase topology could be used for comparison. In order to obtain a comparable wave position, we try to fix the position of the first vortex in the wake. The reference phase angle was chosen to obtain the first vortex center of the OPD 1 modes r0 and r2 in the same position x = 1.6 – marked by a red circle in Fig. 7. Then, OPD 2 is locked at x = 2.6, while OPD 3 is at x = 1.46, see Figs. 8 and 9.

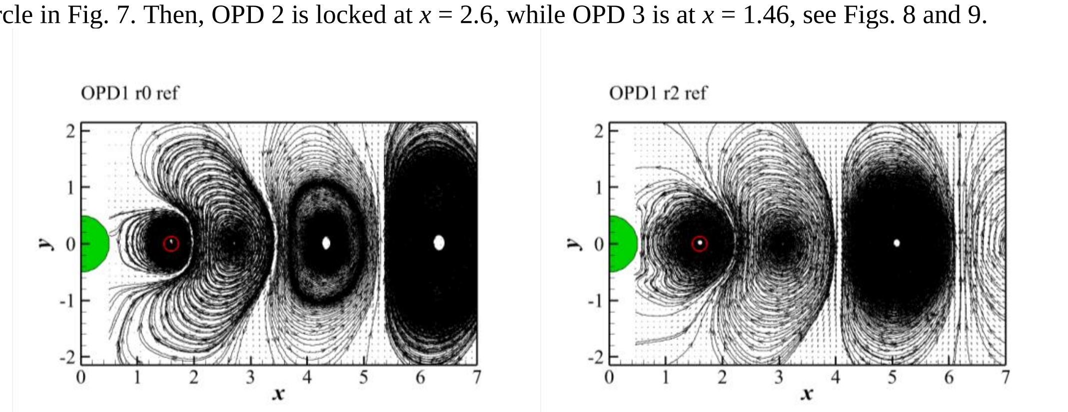

Figure 7: The OPD 1 comparison (smooth surface left, rough right)

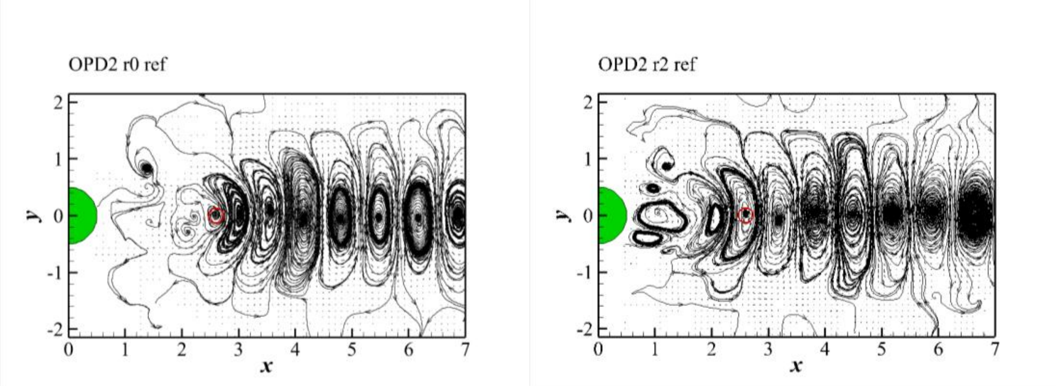

Figure 8: The OPD 2 comparison (smooth surface left, rough right)

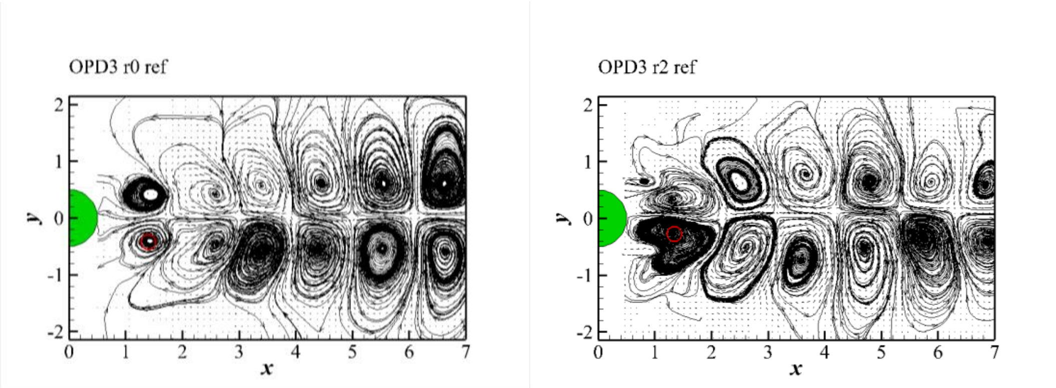

Figure 9: The OPD 3 comparison (smooth surface left, rough right)

Tables 1, 2, and 3 show vortex center *x*-positions for OPD 1, 2, and 3, respectively. Reference vortex positions are in red.

Table 3: Vortices *x*-positions comparison in OPD 1 for the reference phase angle

No.	1	2	3	4
r0	1.6	2.7	4.34	6.32
r2	1.6	3.06	5.07	7.18

Table 4: Vortices *x*-positions comparison in OPD 2 for the reference phase angle

No.	1	2	3	4	5	6	7	8
r0	2.6	3.04	3.55	4.15	4.78	5.47	6.19	6.88
r2	2.6	3.18	3.84	4.5	5.19	5.88	6.65	7.39

Table 5: Vortices *x*-positions comparison in OPD 3 for the reference phase angle

No.	1	2	3	4	5	6
r0	1.46	2.6	3.39	4.44	5.54	6.63
r2	1.46	2.49	3.68	4.8	5.88	6.85

Surface roughness affects the flow topology in the wake, including its dynamics. However, the flow topology is qualitatively unchanged; there are only minor differences in the details.

The vortex spacing in all three dominant OPD modes is increased for the rough surface. This finding is consistent with the lower frequency in the rough case – see Tab. 2.

4 Conclusions

An experimental investigation of the wake behind a circular cylinder at a subcritical Reynolds number of approximately 5 000 was conducted to assess the influence of surface roughness on vortex shedding characteristics. Planar PIV measurements were performed for a smooth cylinder and for a cylinder with uniformly distributed sand-grain roughness.

The results show that surface roughness significantly modifies the mean wake structure by reducing the extent of the recirculation region immediately downstream of the cylinder and increasing turbulence intensity in the near wake. Despite the relatively low Reynolds number, roughness-induced disturbances persisted in the vortex-formation region.

Analysis of the unsteady wake using Oscillation Pattern Decomposition revealed systematic reductions in the Strouhal number for the rough cylinder compared with the smooth reference case. The dominant vortex-shedding mode and its higher harmonics exhibit increased streamwise spacing of vortical structures, indicating a modified wake organization associated with surface roughness.

These findings demonstrate that even in the subcritical regime, where laminar separation dominates, surface roughness has a measurable impact on vortex shedding frequency and wake topology. The results underline the importance of accounting for surface condition when analyzing unsteady wake dynamics and vortex-induced loading on cylindrical structures. The effect is more quantitative than qualitative.

References

[1] A. Roshko, "On the Development of Turbulent Wakes from Vortex Streets," *NACA Report 1191*, 1954.

[2] C. H. K. Williamson, "Vortex dynamics in the cylinder wake," *Annual Review of Fluid Mechanics*, 28, 477–539, 1996.

[3] M.M. Zdravkovich, "Flow Around Circular Cylinders, Volume 1: Fundamentals," *Oxford University Press*, 1997.

[4] C. Norberg, "Flow around a circular cylinder: aspects of fluctuating lift," *Journal of Fluids and Structures*, 15, 459–469, 2001.

[5] C. Norberg, "Fluctuating lift on a circular cylinder: review and new measurements," *Journal of Fluids and Structures*, 2003.

[6] E. Achenbach, "Influence of surface roughness on the cross-flow around a circular cylinder," *Journal of Fluid Mechanics*, 46(2), 321–335, 1971.

[7] W. Chen, et al., "Numerical simulation of surface roughness effects on the vortex-induced vibration of a circular cylinder at a subcritical Reynolds number of 3900," J*ournal of Ocean Engineering and Science*, 2022.

[8] M. Raffel, C. E. Willert, F. Scarano, C. J. Kähler, S. T. Wereley, & J. Kompenhans, "Particle image velocimetry: a practical guide," *Springer*, 2018.

[9] V.Uruba, P. Procházka, "On Harmonic Content of the Wake behind a Circular Cylinder," In: *26th International Conference, ENGINEERING MECHANICS 2020*, pp. 500-503, 2020.

[10] V. Yanovych, D. Duda, V. Uruba, P. Procházka, P. Antoš, "Effect of Cylinder Roughness on Strouhal Number," in *Topical Problems of Fluid Mechanics*, Prague, Czech Republic, pp. 201-207, 2022.

[11] V. Uruba, "Near Wake Dynamics around a Vibrating Airfoil by Means of PIV and Oscillation Pattern Decomposition at Reynolds Number of 65 000," *Journal of Fluids and Structures*, vol. 55, pp. 372-383, 2015.